

Template Instrumentation for “Accurate Constant via Transient Incomplete Separation”

Jean-Luc Rukundo, Sven Kochmann, Tong Ye Wang, Nikita A. Ivanov, J. C. Yves Le Blanc, Boris I. Gorin, and Sergey N. Krylov*



Cite This: *Anal. Chem.* 2021, 93, 11654–11659



Read Online

ACCESS |



Metrics & More



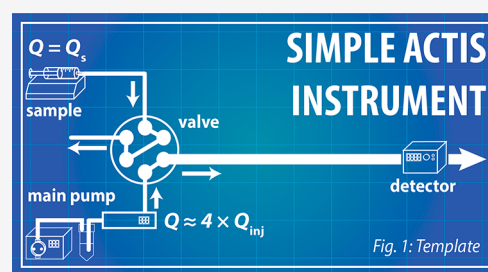
Article Recommendations



Supporting Information

ABSTRACT: Accurate Constant via Transient Incomplete Separation (ACTIS) is a new method for finding the equilibrium dissociation constant K_d of a protein–small molecule complex based on transient incomplete separation of the complex from the unbound small molecule in a capillary. This separation is caused by differential transverse diffusion of the complex and the small molecule in a pressure-driven flow. The advection–diffusion processes underlying ACTIS can be described by a system of partial differential equations allowing for a virtual ACTIS instrument to be built and ACTIS to be studied in silico. The previous in silico studies show that large variations in the fluidic system geometry do not affect the accuracy of K_d determination, thus, proving that ACTIS is conceptually accurate.

The conceptual accuracy does not preclude, however, instrumental inaccuracy caused by run-to-run signal drifts. Here we report on assembling a physical ACTIS instrument with a fluidic system that mimics the virtual one and proving the absence of signal drifts. Furthermore, we confirmed method ruggedness by assembling a second ACTIS instrument and comparing the results of experiments performed with both instruments in parallel. Despite some unintentional differences between the instruments (caused by tolerances in sizes, positions, etc.) and noticeable differences in their respective separagrams, we found that the K_d values determined for identical samples with these instruments were equal. Conclusively, the fluidic system presented here can serve as a template for reliable ACTIS instrumentation.



Proteins (P) can bind small-molecule ligands (L) to form stable noncovalent complexes (PL):



The stability of PL is characterized by the equilibrium dissociation constant (K_d) defined as

$$K_d = [L]_{eq}[P]_{eq}/[PL]_{eq} \quad (2)$$

where $[P]_{eq}$, $[L]_{eq}$, and $[PL]_{eq}$ are equilibrium concentrations of P, L, and PL, respectively. Determining accurate K_d values for PL is important for biology and drug development.^{1,2} However, accurate K_d values cannot be predicted theoretically, and all established methods for finding K_d of PL have inherent sources of inaccuracy.³ Accordingly, K_d values determined by different methods for the same PL complex may differ by orders of magnitude.⁴ Even K_d determined by the same method for the same binding pair can differ drastically.⁵ In the absence of a reference method, K_d values differing by more than 100× may be considered consistent and kept in one data set.⁶ These large inaccuracies in K_d values inevitably lead to a misinterpretation of the experimental results, mistaken conclusions, and misconceptions.⁷

We recently introduced Accurate Constant via Transient Incomplete Separation (ACTIS), a method for finding K_d of PL, which was hypothesized to be free of inherent sources of inaccuracy.⁸ ACTIS is based on a long-known phenomenon of

transient incomplete separation (TIS) of the L from PL in a round-cross-section capillary due to their differential transverse diffusion in a laminar flow with a parabolic velocity profile.^{9,10} In ACTIS, a short plug of an equilibrium mixture of P and L in a buffer solution is injected into a capillary prefilled with the pure buffer solution. The plug is then propagated inside the capillary by a pressure-driven flow of the buffer solution. Different rates of transverse diffusion of PL and L in the laminar flow cause their TIS in the longitudinal direction (Figure 1A), resulting in a separagram containing two unresolved peaks: a nondiffusive peak for PL and a diffusive peak for L.^{9,10} To determine K_d , TIS is performed for a series of equilibrium mixtures (EMs) with a constant concentration of L and varying concentration of P, producing a set of separagrams (Figure 1B). The cumulative signal of protein-bound and protein-unbound L is used to build a classic binding isotherm “fraction of free L versus the concentration of P”, which reveals the value of K_d (Figure 1C).³

Received: May 11, 2021

Accepted: August 6, 2021

Published: August 19, 2021



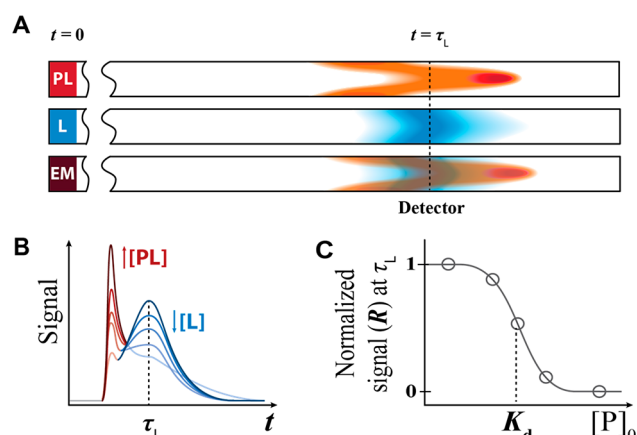


Figure 1. Simplified schematic of determining K_d by ACTIS. (A) A short plug of the equilibrium mixture (EM) of P and L, containing free P, free L, and the complex PL, is pressure-propagated through a capillary. Differences in rates of transverse diffusion of PL and L cause their longitudinal separation. (B) Longitudinal separation results in two unresolved peaks: a nondiffusive peak associated with PL and a diffusive peak associated with L. A cumulative signal from L and PL is measured at time τ_L , corresponding to the maximum of the diffusive peak; this is the characteristic time of transverse diffusion of L. The signal is measured at a constant concentration of L and varied concentrations of P. (C) A binding isotherm “normalized signal at time τ_L vs the total protein concentration $[P]_0$ ” is built, from which the value of K_d is obtained. R is the fraction of free ligand obtained from the normalized signal. This figure is adapted with permission from ref 8. Copyright 2020 ACS.

ACTIS is a deterministic method, that is, the advection-diffusion processes that ACTIS is based on can be described by a system of partial differential equations with fully defined initial and boundary conditions. The deterministic nature of ACTIS allowed us to create a virtual ACTIS instrument *in silico* and study the accuracy of ACTIS by computer modeling, thus, avoiding extremely laborious and often unfeasible physical studies.⁸ This study proved that the accuracy of ACTIS was not affected by large variations in the geometry of the fluidic path and the parameters characterizing the flow. The *in silico* study led to several important conclusions. The initial understanding was that a physical ACTIS instrument had to support ideal conditions such as (i) a cylindrical shape of the initial sample plug, (ii) a parabolic flow-velocity profile, and (iii) the absence of ramp time in the pressure pulse.⁸ Maintaining such ideal conditions would require a complex ACTIS instrument and would not leave flexibility with fluidic path design. The invariance of accuracy demonstrated *in silico* suggests that an ACTIS instrument can be much simpler than it was thought initially.³ Furthermore, it suggests that the

design of the fluidic system can be changed (if needed) without concerns that the accuracy could be affected. Finally, the conceptual accuracy of ACTIS allows the developers to focus on potential instrumental sources of inaccuracy, such as signal drifts caused by run-to-run sample carryover and long-term operation instability of instrument components. This technical note is solely focused on designing such a simple and stable fluidic system for ACTIS, which will serve as a template for any future ACTIS instrumentation.

Here we report on (i) constructing a physical ACTIS instrument that mimics the previously reported simple virtual instrument⁸ and (ii) proving the stability of its operation. The fluidic system of this instrument was coupled with a fluorescence detector. Bovine serum albumin (BSA) and fluorescein were the protein and small molecule for binding of which the K_d value was measured. This molecular pair was chosen as the one for which our original ACTIS measurements were done to reveal the K_d range of 12–28 μM ³ and for which there is a relatively narrow consensus range of K_d values of 10–70 μM found in the literature.^{11–13} We found no significant signal drifts in this ACTIS instrument. We then assembled the second ACTIS instrument and run experiments in parallel on the two instruments on different days by different operators to prove the instrumental ruggedness of the method. The K_d values obtained for the same samples with the two instruments deviated by no more than 10%. Our results suggest that the simple fluidic system presented here can serve as a reliable template for ACTIS instrumentation allowing for ACTIS research on practical applications of this new method for K_d determination in protein-small molecule binding studies.

MATERIALS AND METHODS

Reagents and Solutions. All reagents were obtained from Sigma-Aldrich (Oakville, Ontario, Canada). The binding pair of a protein and small-molecule ligand used here was bovine serum albumin (BSA, catalog A2514) and fluorescein sodium salt (catalog F2456). New BSA solutions of 10 concentrations were prepared prior to each ACTIS experiment and used to prepare new EMs. The same stock solution of 1 μM fluorescein was used throughout the study. A single buffer, 30 mM ammonium acetate, pH 7.5, was utilized to prepare all solutions and used as the sample propagation buffer; accordingly, we simply refer to it as the buffer.

Protein–ligand EMs were prepared by mixing appropriate volumes of working solutions of P and L and incubating for 1 h before the start of ACTIS runs (longer incubation was shown not to change the determined value of K_d suggesting that 1 h was sufficient to approach equilibrium in the binding reaction (eq 1)). All EMs had identical total ligand concentration $[L]_0 = 100$ nM, unless otherwise stated, while the total protein

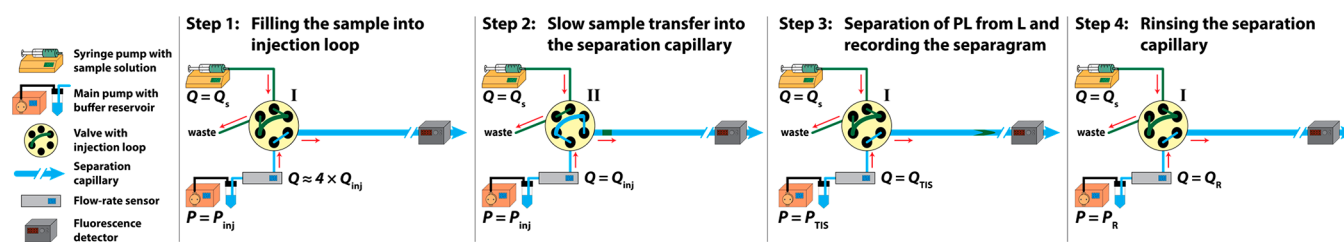


Figure 2. Components of the ACTIS setup and four steps of a single run in an ACTIS experiment, which produces a single separagram. The two valve positions are indicated by Roman numbers I and II. Letters P and Q show pressures and flow rates, respectively. The red arrows show the directions of the flows. See the text for more details.

concentrations in the EMs, $[P]_0$, varied within 4 orders of magnitude: from 0.1 μM to 1 mM. All sample handling and measurements were carried out at a room temperature of 20 ± 2 °C. Identical samples were utilized when experiments were conducted with two ACTIS setups in parallel.

Fluidic Setup Components. The two ACTIS instruments used in this study had similar fluidic systems shown schematically in Figure 2. The fluidic systems included: a pump (called here the main pump, model “AF1”, Elveflow, Paris, France), a syringe pump (interchangeably called the sample pump, model “Pump 11 Elite”, Harvard Instruments, Holliston, U.S.A.), a high-pressure 6-port 2-position valve (Vici Valco, Houston, TX, U.S.A.), a flow rate sensor (model “Coriolis Flow Sensor”, Elveflow, Paris, France), and a fluorescence detector (see the details in the next section). Fused-silica capillaries (Molex, Phoenix, AZ, U.S.A.) were used for both the separation capillary (200 μm ID, 80 cm length) and the injection loop (100 μm ID, 13 cm length; 1 μL volume). Fittings and connectors were from SciPro Technologies (Sanborn, U.S.A.). The main pump could be operated in both pressure-control and flow-rate-control modes. We found that this pump produced a more stable flow when operated in the pressure-control mode, while the flow rate was the parameter to be controlled. Therefore, the pump pressure P was changed to obtain a desired flow rate Q measured by the flow-rate sensor (see the numerical details below). The syringe pump controlled the flow rate of the sample inflow into the valve at a constant level of Q_s (see the numerical details below). No special effort was taken to make the fluidic systems of the two ACTIS instruments identical. Accordingly, there were likely some minor variations allowing us to test if such variations could affect K_d determination significantly. Photographs of both instruments are shown in Figure S1.

Fluorescence Detection. Laser-induced-fluorescence detectors from commercial CE instruments (model “PACE-MDQ”, SCIEX, Concord, Ontario, Canada) were used for the two ACTIS setups. Both utilized 488 nm solid-state lasers (Model W488–08PM, Pavilion Integration Corporation, San Jose, CA, U.S.A.). Fluorescence signals were detected through transparent windows (detection windows) in the uncoated (nontransparent) capillaries; the detection windows were located 60 cm from the capillary inlet. These detectors use ball lenses to collect fluorescence light. The lens is placed in close proximity to the capillary. Focusing is very sensitive to the lens position and it may differ from detector to detector. No effort was taken to make focusing identical for the two detectors.

Differences between the ACTIS Instruments. The two ACTIS instruments used in this study were assembled of similar parts and in a similar way. However, the instruments had unavoidable differences caused, in particular, by (i) manufacturer-allowed variations in capillary diameters (200 ± 6 μm and 100 ± 4 μm), (ii) variations in lengths of custom-made capillary cuts (± 3 mm), (iii) manufacturer-allowed variations in the ball-lens position in the fluorescence detection (unspecified), (iv) pressure variance of the main pump (up to 20% of applied pressure), and so on. We made no effort to eliminate the variances or account for them due to the proven robustness of ACTIS to instrument and flow geometry.⁸ Another reason for not attempting to minimize the differences was to test and confirm the instrument robustness to variations in the detection system.

ACTIS Experiment. The same experimental procedure was used for both ACTIS instruments. The fluidic setup was pre-filled with the buffer before the first run in a run series with one concentration of the protein. A standard ACTIS experiment included four steps facilitated by two positions (I and II) of the valve and two pumps (Figure 2). In Step 1, the valve was in position I, and the injection loop was filled continuously with the sample using a syringe pump at a flow rate of $Q_s = 20$ $\mu\text{L}/\text{min}$. The main pump was running at a pressure P_{inj} identical to that of the next step. In Step 2, the valve was switched to position II, and the sample plug was slowly transferred from the injection loop to the separation capillary by the main pump for 24 s at a pressure P_{inj} set at a level that produced a flow rate of $Q_{\text{inj}} = 5$ $\mu\text{L}/\text{min}$. When the transfer ended, the sample plug was one sample–plug distance from the separation-capillary inlet to ensure a complete sample transfer to the separation capillary. In Step 3, the valve was switched back to position I, and the sample plug was propagated inside the capillary for 48 s by the main pump at a pressure of P_{TIS} that produced a flow rate of $Q_{\text{TIS}} \approx 57$ $\mu\text{L}/\text{min}$. Q_{TIS} was chosen to allow efficient TIS of L from the PL (see Note S1 for calculations). In Step 4, the valve remained in position I, and the separation capillary was rinsed with the buffer, which was pumped by the pressure pump at a flow rate of $Q_{\text{rinse}} \approx 250$ $\mu\text{L}/\text{min}$ for 1 min allowing for 10 volumes of the separation capillary to pass through the fluidic system. The four-step experimental run took approximately 2.3 min.

Before injecting a sample with a different protein concentration, the fluidic system was thoroughly rinsed with the buffer in a final rinsing step (see Note S2 for details). For this “between-sample” rinsing step, a syringe containing the buffer was mounted on a syringe pump set to run at a flow rate of 80 $\mu\text{L}/\text{min}$, and the main pump kept injecting the buffer at a pressure corresponding to a flow rate of 80 $\mu\text{L}/\text{min}$; the valve was in position II. The buffer was pumped through two ports of the valve by repeatedly switching the valve between positions I and II. For each switch, the valve spent 1 s in position I (the time for the injection loop to be filled once and) and 2 s in position II (allowing the injection of two volumes of the injection loop into the separation capillary). This switching mimicked the sample-injection and TIS steps of the ACTIS experiment allowing the buffer to attain all the parts inside the fluidic system where the sample might have been retained or adsorbed. During this rinsing, nine volumes of the separation capillary passed through the fluidic system. This rinsing step took approximately 4 min.

A total of 3–5 ACTIS runs were performed for each concentration of the protein to establish the mean value and standard deviation. An ACTIS experiment with 10 protein concentrations along with all the rinsing steps took approximately 3.5 h.

Determination of K_d . The values of K_d were determined in two steps. First, we built a classic binding isotherm “fraction of free ligand R versus protein concentration $[P]_0$ ” where R is defined as

$$R = \frac{[L]_{\text{eq}}}{[L]_{\text{eq}} + [PL]_{\text{eq}}} = \frac{[L]_{\text{eq}}}{[L]_0} \quad (3)$$

Second, we conducted a nonlinear fitting of the experimental dependence of R on $[P]_0$ with the theoretical one:

$$R = -\frac{K_d + [P]_0 - [L]_0}{2[L]_0} + \sqrt{\left(\frac{K_d + [P]_0 - [L]_0}{2[L]_0}\right)^2 + \frac{K_d}{[L]_0}} \quad (4)$$

in which K_d is a fitting parameter, into the experimental isotherm.² To obtain the R values, we performed TIS on each of the 10 EMs (each with a different total concentration of the protein $[P]_0$) by running each EM in the ACTIS instrument as described in the previous section. At least three replicated runs were made for each EM, and a signal value for each run was obtained by averaging points within a time window around the diffusive-peak-maximum position. This position corresponds approximately to the characteristic time of transverse diffusion of the protein-unbound ligand.³ We took a total time window width corresponding to 8% of the diffusive-peak-maximum position, that is, $\pm 4\%$ around this position. The time window used in the determination of signal values was selected from the first EM at $[P]_0 = 0.1 \mu\text{M}$ and applied subsequently to all other EMs at other $[P]_0$ values. The signal values obtained from the replicated runs were used to find an average signal value, from which the values of R and corresponding standard deviations (obtained through simple error propagation) were calculated using equations described in a previous ACTIS publication.³ The K_d value and its standard deviation were then obtained by fitting the experimental dependence of R versus $[P]_0$ with their theoretical relationship by performing a nonlinear fitting using the Levenberg–Marquardt algorithm in the OriginPro software. The standard deviation of K_d values indicates the goodness of the nonlinear fit.

RESULTS AND DISCUSSION

An ACTIS instrument has a minimum fluidic setup with the sample pump, the main pump, the injection loop, the separation capillary, the multipoint valve, and the flow-rate sensor (Figure 2). The deterministic nature of ACTIS allowed us to assess its accuracy earlier by using a virtual ACTIS instrument built in COMSOL.⁸ Our *in silico* study revealed that ACTIS accuracy was not influenced significantly by large variations in the parameters of the fluidic setup: the radius of the separation capillary, the radius and length of the injection loop, and the ramp time of the main pump.⁸ This invariance of accuracy is important because it gives flexibility in instrument design, and guarantees that the accuracy will not be affected by deviations in the performance parameters of the key instrument components from their nominal values provided by the manufacturer. Specifically, this robustness of accuracy suggests that a very elaborate fluidic system used by us in the proof-of-concept work to achieve a near-cylindrical starting sample plug is not necessary.^{3,8} Therefore, we assembled a physical mimic of the simple fluidic setup evaluated in the *in silico* study (see Materials and Methods for details).

ACTIS is a titration-like method with no internal standard. Therefore, the high repeatability of separagrams obtained from injecting identical samples is imperative for high accuracy in K_d determination. Two conditions must be satisfied to achieve run-to-run repeatability: (i) no sample carryover and (ii) long-term operation stability of all components of the instrument, specifically the main pump and the detector. Sample carryover and instrument instabilities can cause gradual changes in separagrams which will inevitably lead to systematic errors in K_d values. Observing repeatability of separagrams and signal stability would indicate that both conditions are satisfied, that is, there is neither sample carryover nor long-term operation instability of instrument components.

The stability of the ACTIS instrument was proven by conducting 60 consecutive runs of a fluorescein solution for approximately 2 h. The resulting separagrams and dependencies of the peak parameters (height and position) on run number for the first ACTIS instrument are shown in Figure 3A, left and right panels, respectively. The dependencies show

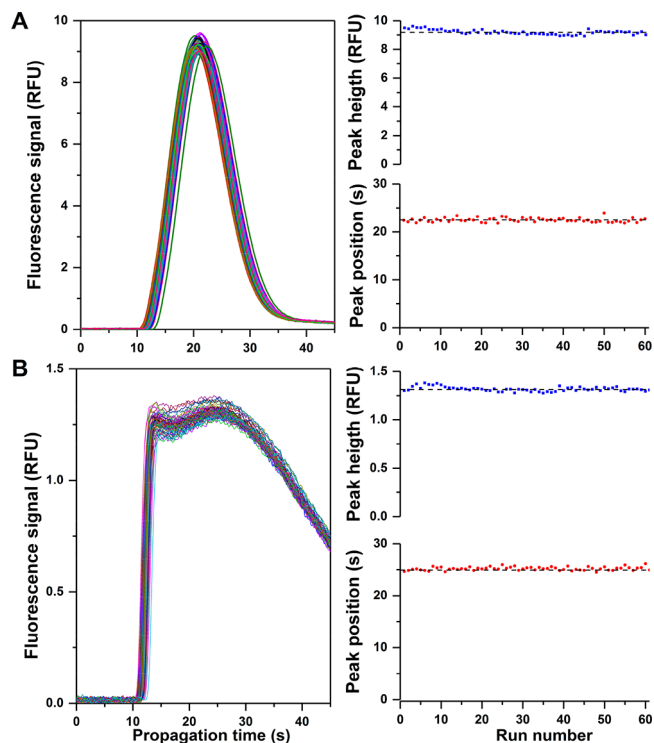


Figure 3. Repeatability of separagrams in 60 runs of 100 nM fluorescein (A) and a mixture of 100 nM fluorescein with 0.5 mM BSA (B). The left panels show separagrams, while the right panels show the dependencies of the height and position of the diffusive peak on the run number.

approximately 5% decrease in peak height toward a stable value during the first 10 runs and only a random variation (2% RSD) in peak position. The initial change in peak height is likely associated with laser's and/or photomultiplier's slowly reaching their stable operation condition, for example, the steady-state temperature. The absence of any noticeable drifts in peak position suggests very stable operation of the main pump. To increase the stringency of this test, we then ran a mixture containing 0.5 mM concentration of BSA along with fluorescein. BSA is a highly adsorbing protein and the 0.5 mM concentration used is among the highest concentrations ever used in *in vitro* experiments. This mixture was a perfect sample to challenge the ACTIS instrument and check if there was any sample carryover caused by protein adsorption. We conducted 60 consecutive runs of this mixture over a period of approximately 2 h (on a different day) and found highly repetitive separagrams (Figure 3B, left). Heights and positions of the diffusive peak were measured and presented as functions of run number (Figure 3B, right). The dependencies were similar to those of pure fluorescein (Figure 3A, right), leading to similar conclusions about the performance of the detector and the main pump: minor releveling in the detector response and no noticeable instability in the main pump pressure.

The observed stability of separagrams for samples without and with the protein indicates that there was no sample carryover and that the pump and detector could support stable instrument operation. Specifically, these results suggest that the rinsing procedure used by us will be adequate for most other proteins as BSA is a highly adsorbing protein.^{13,14} In the unlikely event that protein adsorption for another protein is observed, the inner surface of the injection loop and the separation capillary can be coated to suppress protein adsorption.¹⁵

Finally, we conducted a comprehensive test of ACTIS ruggedness. We assembled the second ACTIS instrument and ran ACTIS experiments on two instruments by two operators in parallel using identical samples for every experimental set. The instruments were built of similar components, but no specific effort was undertaken to make the fluidic systems and detectors identical. As a result, the instruments likely differed in their ratios of the capillary length to flow velocity due to finite tolerance of cutting capillary and setting the flow rate via a pressure pump. However, ACTIS is robust to variations in this parameter;⁸ accordingly, we did not dedicate time to perfect this parameter. The instruments also likely differed in focusing performance of the commercial detectors' optics due to the specifics of ball lenses.¹⁶ These unintentional and hardly avoidable differences cumulatively were the reason for significant differences in the relative heights and positions of the nondiffusive peak (the left-hand side peak) between the two instruments (Figure 4, left panels). The same differences

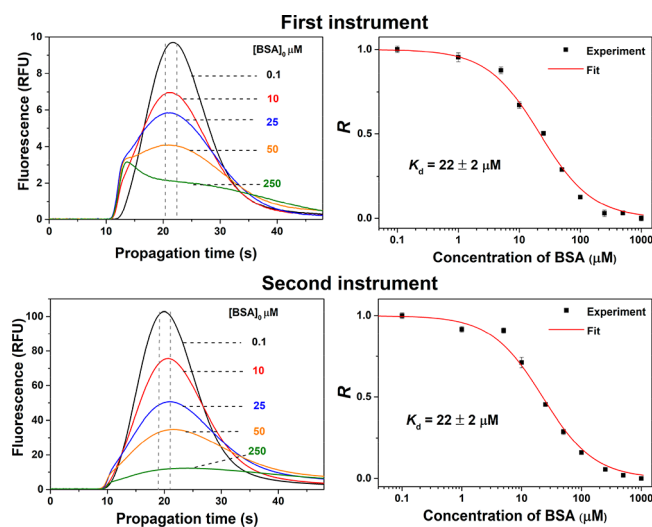


Figure 4. Robustness of K_d determination by ACTIS demonstrated with two ACTIS instruments used to run identical samples containing 100 nM fluorescein and varying concentrations of BSA. The left panels show representative separagrams (one of five for each BSA concentration), and the right panels show the corresponding binding isotherms. R is a fraction of unbound fluorescein.

were observed between the results obtained with these instruments in all the following experiments (Figures S2–S7). Importantly, these differences in the separagram shapes did not lead to deviations in the K_d values between the two instruments. All experiments performed in parallel with the two instruments returned K_d values equal within limits of precision provided that identical samples were used (Figure 5). New solutions were prepared every day and day-to-day variations were more significant; the largest K_d value was 28

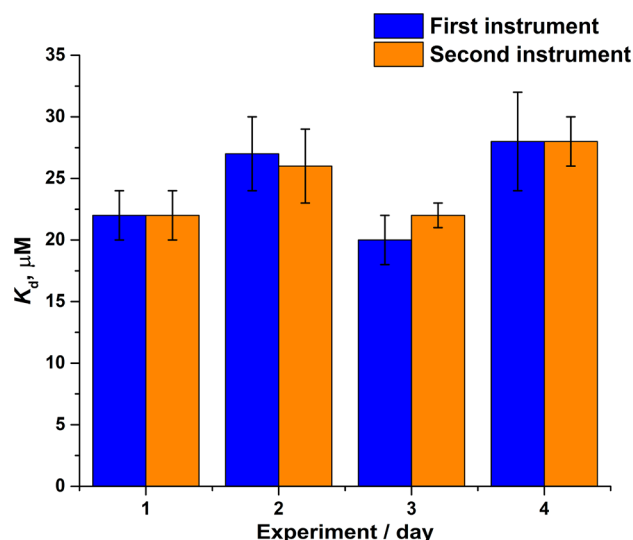


Figure 5. Ruggedness of K_d determination with two ACTIS instruments with new samples prepared for each experiment; identical samples were used for each of the two instruments in each experiment.

μM and the smallest value was 20 μM . Our results clearly show the robustness and ruggedness of ACTIS experiments suggesting that this simple ACTIS instrumentation can support accurate K_d determination.

CONCLUDING REMARKS

There are two major aspects in ACTIS: accuracy and reproducibility. Accuracy cannot be proven experimentally for any K_d measurement method due to fundamental reasons.⁸ However, accuracy can be proven in silico for a deterministic method. Since ACTIS is a deterministic method, we previously conducted an in silico study and proved that ACTIS accuracy would not be affected by differences in the shape of the geometry of the fluidic path and parameters of the flow, provided that the instrument is stable.⁹ The requirement of instrument stability is paramount, but this stability cannot be tested in silico. In this study, we proved that the presented experimental setup is stable and, thus, guarantees accurate K_d measurements. It is critical for any newly assembled ACTIS instrument to be tested for stability by conducting an experiment similar to the one presented in Figure 3 since an unstable instrument will cause signal drifts and, thus, inaccurate K_d measurements.

We present a simple ACTIS instrument that supports stable operation, repeatability, and reproducibility. The proven stability of ACTIS instrumentation translates into high accuracy of K_d determination. Our results with two ACTIS instruments suggest that ACTIS instrumentation is responsible for a small inaccuracy (approximately 10%) in K_d determination. It should be noted that the accuracy of the determined K_d values depends on the accuracy of protein concentrations used. Errors in protein concentrations are the most probable source of inaccuracy in ACTIS experiments manifested in K_d differences between experiments performed with new samples. The influence of inaccurate protein concentration will be more significant for unstable proteins. To address this problem, one can assess the applicability to ACTIS of a double-titration procedure, in which both the protein concentration in the stock solution and the K_d value are determined.¹⁷ The

presented fluidic system can be combined not only with fluorescence detection but also with any other “point-detection” system including mass spectrometry. ACTIS coupled with mass spectrometry provides a means of studying interactions of unlabeled molecules as we demonstrated earlier.³ The absolute lower limit of K_d values measured by ACTIS is defined by the LOQ for the ligand and is in the nanomolar concentration range for both fluorescence and mass spectrometry detection. The upper limit is defined by protein solubility and can be assumed to be 0.1 \times solubility for accurate K_d determination. To conclude, the simple fluidic setup of the ACTIS instrument reported in this work can be used to accurately and reliably determine K_d values, and we foresee ACTIS being used as a new reference method for K_d measurement.

■ ASSOCIATED CONTENT

SI Supporting Information

The Supporting Information is available free of charge at <https://pubs.acs.org/doi/10.1021/acs.analchem.1c02007>.

Flow Rate for Transient Incomplete Separation (Note S1, Scheme 1); Between-sample rinsing step (Note S2, Scheme 1); Photographs of the two ACTIS instruments (Figure S1); Determination of K_d value of the BSA–Fluorescein Pair on Day 2 (Figure S2); Determination of K_d value of the BSA–Fluorescein Pair on Day 3 (Figure S3); Determination of K_d value of the BSA–Fluorescein Pair on Day 4 (Figure S4); Determination of K_d value of the BSA–Fluorescein Pair on Day 5 (Figure S5); Repeatability of the ACTIS Separagrams for the BSA–Fluorescein Complex, Day 1, Instrument 1 (Figure S6); Repeatability of the ACTIS Separagrams for the BSA–Fluorescein Complex, Day 1, Instrument 2 (Figure S7) (PDF)

■ AUTHOR INFORMATION

Corresponding Author

Sergey N. Krylov – Department of Chemistry and Centre for Research on Biomolecular Interactions, York University, Toronto, Ontario M3J 1P3, Canada; orcid.org/0000-0003-3270-2130; Email: skrylov@yorku.ca

Authors

Jean-Luc Rukundo – Department of Chemistry and Centre for Research on Biomolecular Interactions, York University, Toronto, Ontario M3J 1P3, Canada; orcid.org/0000-0003-3626-2515

Sven Kochmann – Department of Chemistry and Centre for Research on Biomolecular Interactions, York University, Toronto, Ontario M3J 1P3, Canada; orcid.org/0000-0001-7423-4609

Tong Ye Wang – Department of Chemistry and Centre for Research on Biomolecular Interactions, York University, Toronto, Ontario M3J 1P3, Canada; orcid.org/0000-0001-9462-7194

Nikita A. Ivanov – Department of Chemistry and Centre for Research on Biomolecular Interactions, York University, Toronto, Ontario M3J 1P3, Canada; orcid.org/0000-0002-0842-6626

J. C. Yves Le Blanc – SCIEX, Concord, Ontario L4K 4 V8, Canada; orcid.org/0000-0002-3801-3590

Boris I. Gorin – Eurofins CDMO Alphora, Mississauga, Ontario L5K 1B3, Canada; orcid.org/0000-0003-1500-5392

Complete contact information is available at: <https://pubs.acs.org/doi/10.1021/acs.analchem.1c02007>

Author Contributions

The manuscript was written through contributions of all authors, and all authors have given approval to the final version of the manuscript before the submission.

Notes

The authors declare no competing financial interest.

■ ACKNOWLEDGMENTS

This work was supported by the Natural Sciences and Engineering Research Council of Canada (Grant SPGP 521331-2018).

■ REFERENCES

- (1) Hoare, S. R.; Fleck, B. A.; Williams, J. P.; Grigoriadis, D. E. *Drug Discovery Today* **2020**, *25*, 7–14.
- (2) Velázquez Campoy, A.; Freire, E. *Biophys. Chem.* **2005**, *115*, 115–124.
- (3) Sisavath, N.; Rukundo, J.-L.; Le Blanc, J. C. Y.; Galievsky, V. A.; Bao, J.; Kochmann, S.; Stasheuski, A. S.; Krylov, S. N. *Angew. Chem., Int. Ed.* **2019**, *58*, 6635–6639.
- (4) Bottari, F.; Daems, E.; de Vries, A.-M.; Van Wielendaele, P.; Trashin, S.; Blust, R.; Sobott, F.; Madder, A.; Martins, J. C.; De Wael, K. *J. Am. Chem. Soc.* **2020**, *142*, 19622–19630.
- (5) Fielding, L. *Prog. Nucl. Magn. Reson. Spectrosc.* **2007**, *51*, 219–242.
- (6) Watzig, H.; Oltmann-Norden, I.; Steinicke, F.; Alhazmi, H. A.; Nachbar, M.; El-Hady, D. A.; Albishri, H. M.; Baumann, K.; Exner, T.; Bockler, F. M.; El Deeb, S. *J. Comput.-Aided Mol. Des.* **2015**, *29*, 847–865.
- (7) Hulme, E. C.; Trevethick, M. A. *Br. J. Pharmacol.* **2010**, *161*, 1219–37.
- (8) Rukundo, J.-L.; Le Blanc, J. C. Y.; Kochmann, S.; Krylov, S. N. *Anal. Chem.* **2020**, *92*, 11973–11980.
- (9) Harada, M.; Kido, T.; Masudo, T.; Okada, T. *Anal. Sci.* **2005**, *21*, 491–496.
- (10) Okada, T.; Harada, M.; Kido, T. *Anal. Chem.* **2005**, *77*, 6041–6046.
- (11) Andersson, L.-O.; Rehnstrom, A.; Eaker, D. L. *Eur. J. Biochem.* **1971**, *20*, 371–380.
- (12) Pinger, C. W.; Castiaux, A.; Speed, S.; Spence, D. M. *J. Chem. Educ.* **2018**, *95*, 1662–1667.
- (13) Munson, M. S.; Meacham, J. M.; Locascio, L. E.; Ross, D. *Anal. Chem.* **2008**, *80*, 172–178.
- (14) Scarangella, A.; Soumbo, M.; Villeneuve-Faure, C.; Mlayah, A.; Bonafos, C.; Monje, M. C.; Roques, C.; Makasheva, K. *Nanotechnology* **2018**, *29*, 115101.
- (15) Yu, B.; Liu, P.; Cong, H.; Tang, J.; Zhang, L. *Electrophoresis* **2012**, *33*, 3066–3072.
- (16) Nouadje, G.; Nertz, M.; Verdeguer, P.; Couderc, F. *J. Chromatogr. A* **1995**, *717*, 335.
- (17) Ye, N.; Busch, D. H. *Inorg. Chem.* **1991**, *30*, 1815–1819.

SUPPORTING INFORMATION

Template Instrumentation for “Accurate Constant *via* Transient Incomplete Separation” (ACTIS)

Jean-Luc Rukundo,¹ Sven Kochmann,¹ Tong Ye Wang,¹ Nikita A. Ivanov,¹ J. C. Yves Le Blanc,² Boris I. Gorin,³ and Sergey N. Krylov^{1*}

¹Department of Chemistry and Centre for Research on Biomolecular Interactions, York University, Toronto, Ontario M3J 1P3, Canada;

²SCIEX, Vaughan, Concord L4K 4V8, Canada;

³Eurofins CDMO Alphora, Mississauga, Ontario L5K 1B3, Canada.

Table of Contents Sections

Note S1: Flow Rate for Transient Incomplete Separation	2
Note S2: Between-sample rinsing step	3
Figure S1: Photographs of the two ACTIS instruments.....	4
Figure S2: Determination of K_d Value of the BSA–Fluorescein Pair on Day 2	6
Figure S3: Determination of K_d Value of the BSA–Fluorescein Pair on Day 3	7
Figure S4: Determination of K_d Value of the BSA–Fluorescein Pair on Day 4	8
Figure S5: Determination of K_d Value of the BSA–Fluorescein Pair on Day 5	9
Figure S6: Repeatability of the ACTIS Separagrams for the BSA-Fluorescein Complex, Day 1, Instrument 1	10
Figure S7: Repeatability of the ACTIS Separagrams for the BSA-Fluorescein Complex, Day 1, Instrument 2	11

Additional supplementary files

The following supplementary files can be found on ChemRxiv:

<https://figshare.com/s/0a78ebc58c4aa02bd22d>

File name	Description/Experiment
evaluation.zip	Raw data and evaluation files.

Note S1: Flow Rate for Transient Incomplete Separation

The recording of a separagram started with the beginning of TIS, which, in turn, started when the main pump applied the pressure of P_{TIS} causing the flow rate Q_{TIS} which was near optimum for detecting the diffusive peak. Q_{TIS} was chosen so that the detection time (t_{det}), defined as time of the diffusive peak maximum on the separagram, was approximately equal to the characteristic diffusion time (τ_L) of L:

$$t_{det} \approx \tau_L \quad (S1)$$

where t_{det} was determined with pure L. The characteristic diffusion time is defined as:

$$\tau_L = a^2 / \mu_L \quad (S2)$$

where a is the inner radius of the separation capillary and μ_L is the diffusion coefficient of L.

The above two equations result in the following ratio:

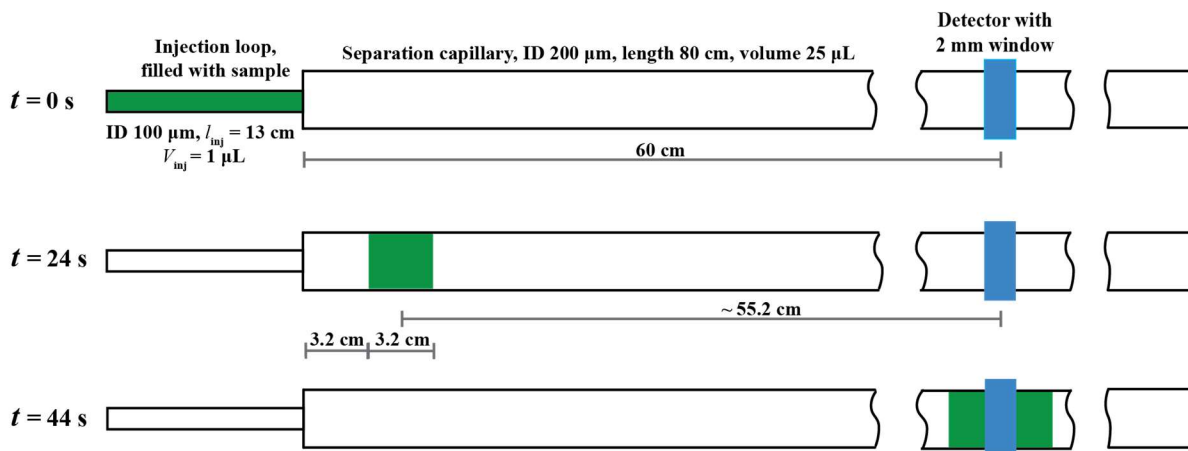
$$l/Q_{TIS} \approx 1/(\pi\mu_L) \quad (S3)$$

where l is the distance between the sample plug and the detection window on the separation capillary after sample transfer into the capillary.

Fluorescein plays a role of L in this study; its diffusion coefficient is $\mu_L \approx 500 \mu\text{m}^2/\text{s}$. The separation capillary has an inner radius of $a = 100 \mu\text{m}$. According to eqs 1 and 2, the detection time will be:

$$t_{det} = 20 \text{ s} \quad (S4)$$

As described in the main text, the sample is transferred from the injection loop to the separation capillary at a flow rate of $5 \mu\text{L}/\text{min}$ for 24 s. The plug length is approximately 3.2 cm; the distance from the capillary inlet to the plug center is approximately 4.8 cm (see the following schematic):



Scheme S1. Geometry of the injection loop and separation capillary.

Since the latter value is much smaller than the distance from the capillary inlet to the detector, we simply assumed that after sample transfer into the separation capillary, the distance between the plug and the detector is

$$l = 60 \text{ cm} \quad (S5)$$

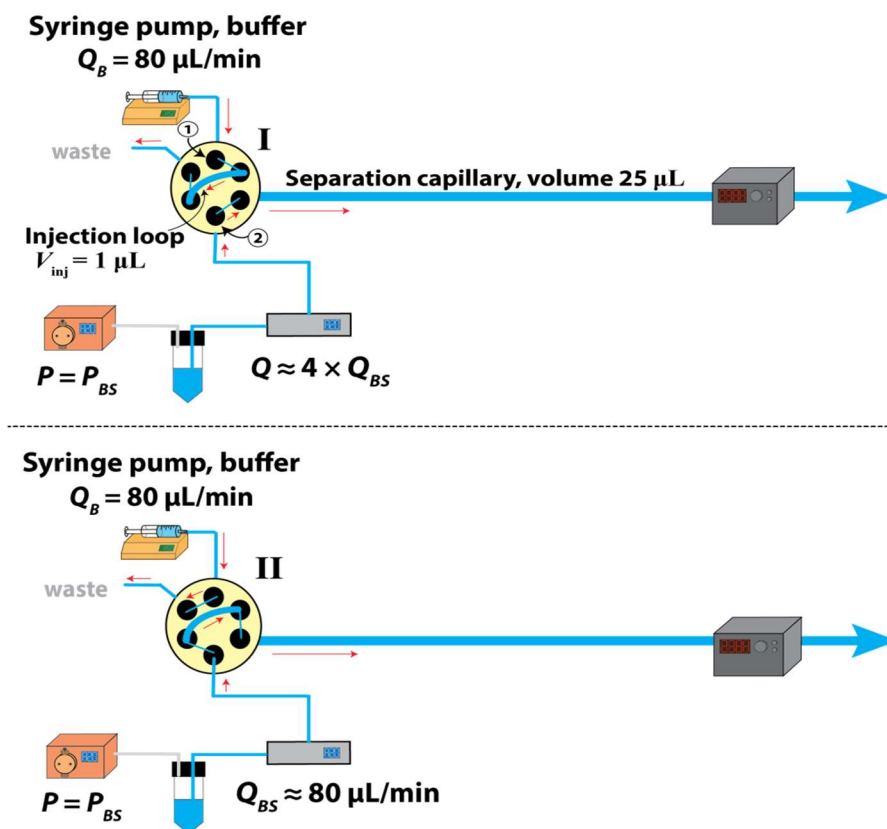
Based on eq. S3, the flow rate was calculated and set to be:

$$Q_{TIS} = 57 \mu\text{L}/\text{min} \quad (S6)$$

Note, that ACTIS is very robust to variations in the flow rate, which allows one to use rough approximations for μ_L and l (see **ref 3** in main text).

Note S2: Between-sample rinsing step

The final rinsing step was performed before injecting a sample with a different protein concentration. A syringe containing the buffer was set on a syringe pump at a flow rate Q_B of $80 \mu\text{L}/\text{min}$, and the main pump injected the buffer at a pressure P_{BS} corresponding to a rinsing flow rate, Q_{BS} , of approximately $80 \mu\text{L}/\text{min}$ at position **II** of the valve (see schematic below). The buffer was pumped through two ports, ports 1 and 2, of the valve by repeatedly switching the valve between positions **I** and **II**. For each switch, the valve stayed in position **I** for 1 sec, the time fill the injection loop volume (V_{inj}) once, and in position **II** for 2 secs injecting $2 \times V_{inj}$ of the buffer into the separation capillary. This switching mimicked the sample-injection and sample propagation steps of the ACTIS experiment allowing the buffer to attain all the parts inside the fluidic system where the sample might have been retained or adsorbed. During this rinsing 80 switches, lasting ~ 4 mins, were done allowing about nine volumes of the separation capillary to pass through the fluidic system.

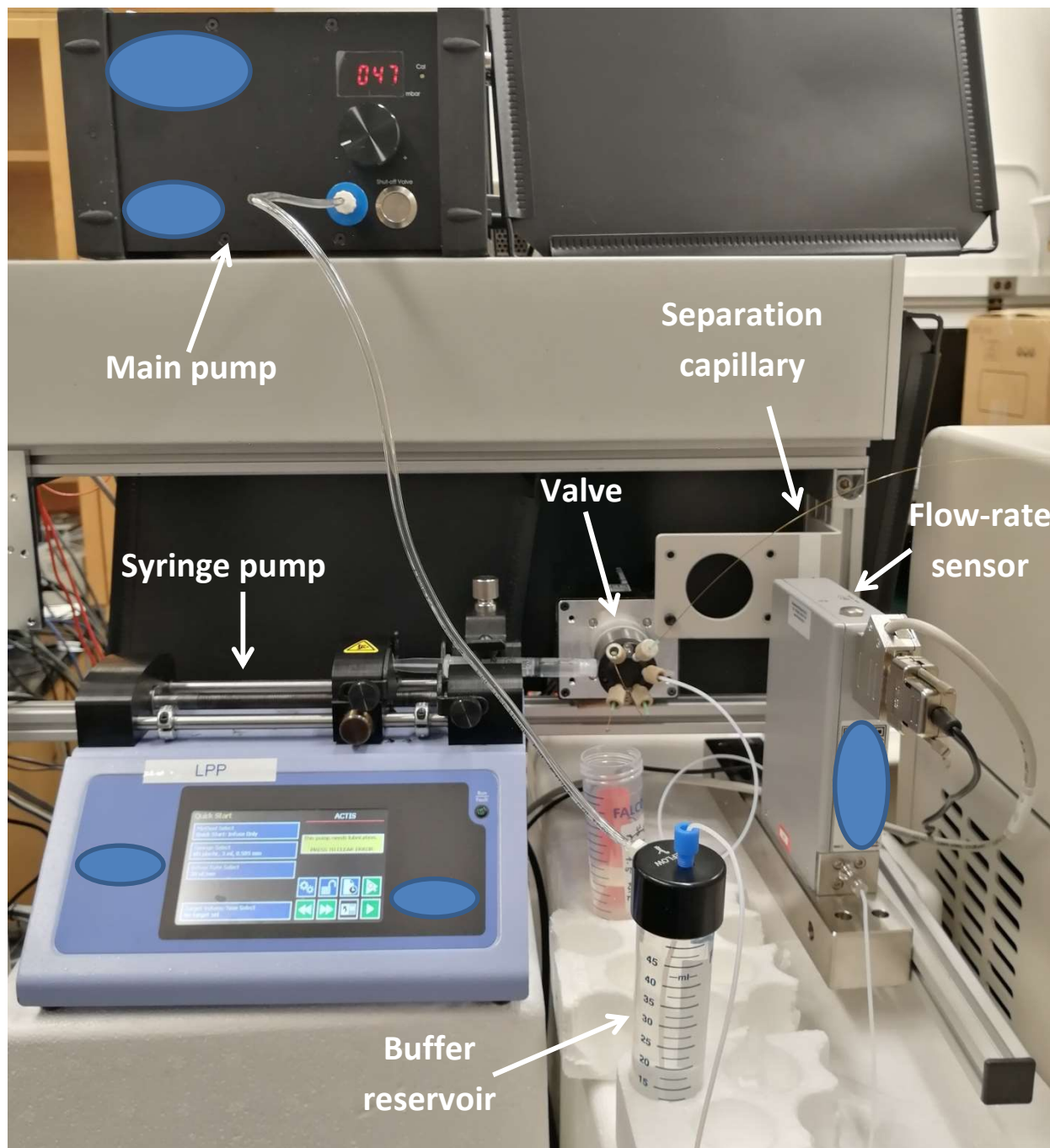


Scheme S2. Flow paths for the final rinsing of the fluidic system.

Figure S1: Photographs of the two ACTIS instruments

Pictures of the first and second ACTIS instruments showing the valve, main pump, syringe pump, flow-rate sensor, and the separation capillary. The detector is to the right of the separation capillary and is not shown for clarity.

First instrument



Second instrument

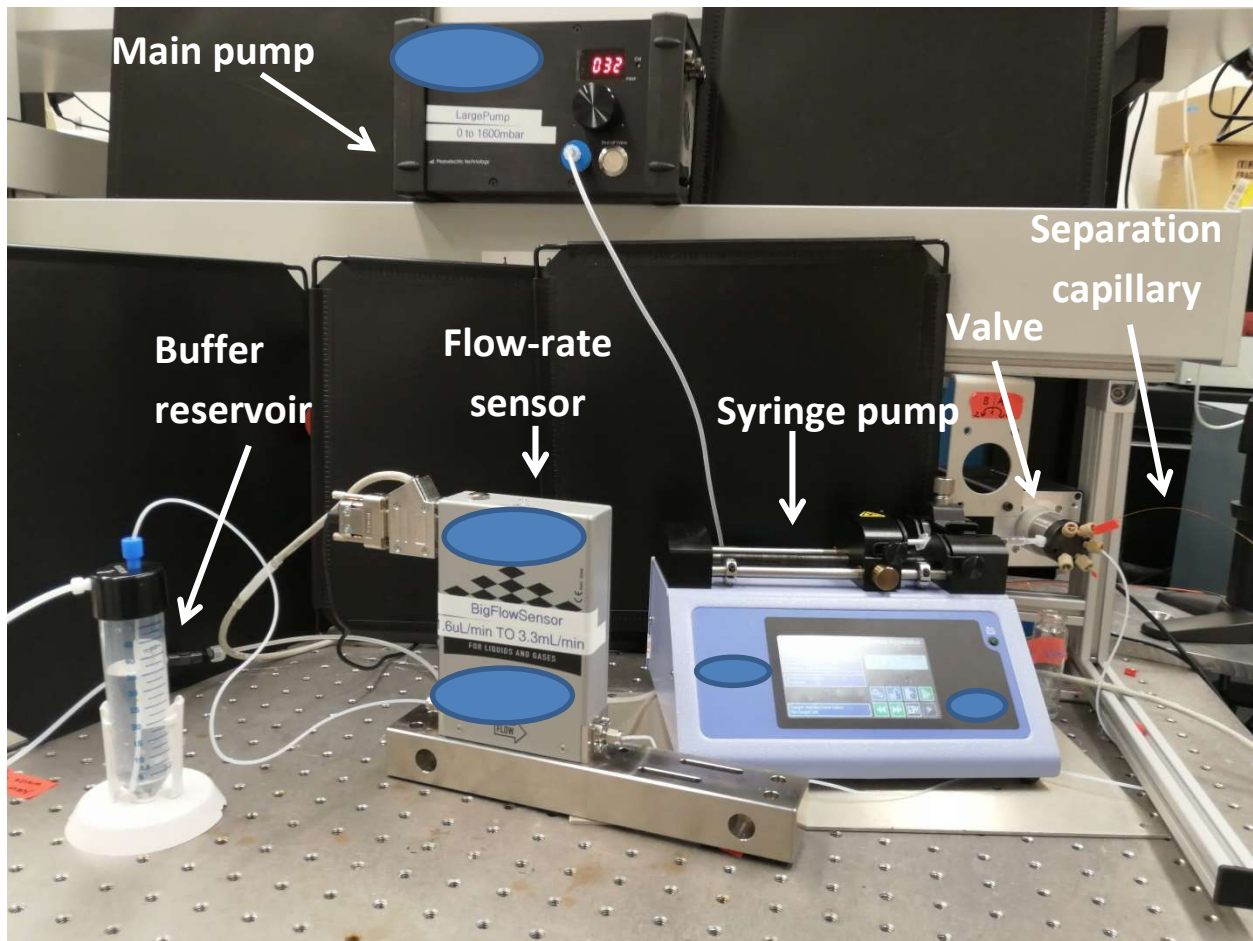


Figure S2: Determination of K_d Value of the BSA–Fluorescein Pair on Day 2

For the parallel experiments, identical samples containing 100 nM fluorescein and different concentrations of BSA were used. The left panels show representative separagrams for each concentration of BSA, and the right panels show the corresponding binding isotherms obtained for all of the separagrams. R is the fraction of unbound fluorescein.

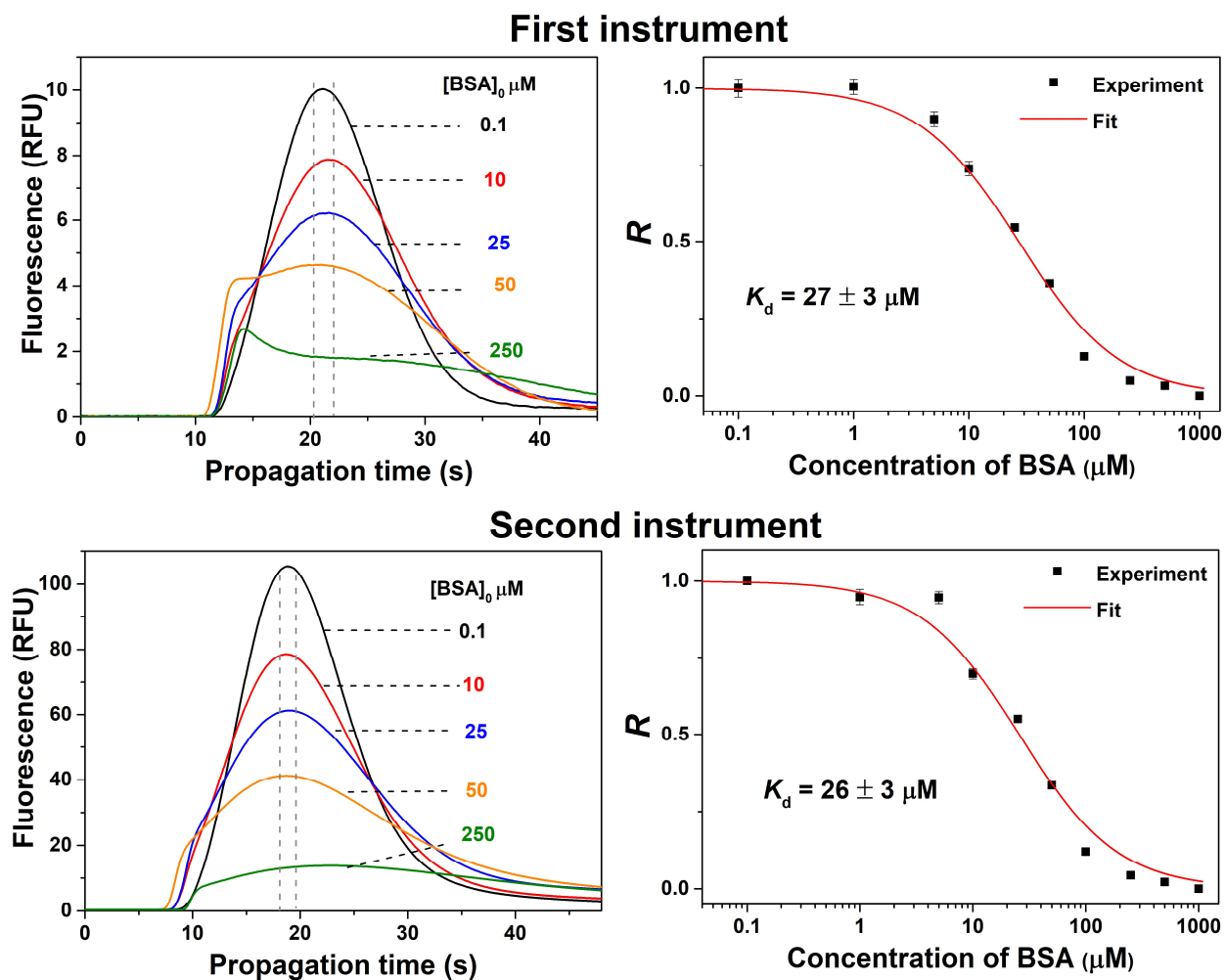


Figure S3: Determination of K_d Value of the BSA–Fluorescein Pair on Day 3

For the parallel experiments, identical samples containing 100 nM fluorescein and different concentrations of BSA were used. The left panels show representative separagrams for each concentration of BSA, and the right panels show the corresponding binding isotherms obtained for all of the separagrams. R is the fraction of unbound fluorescein.

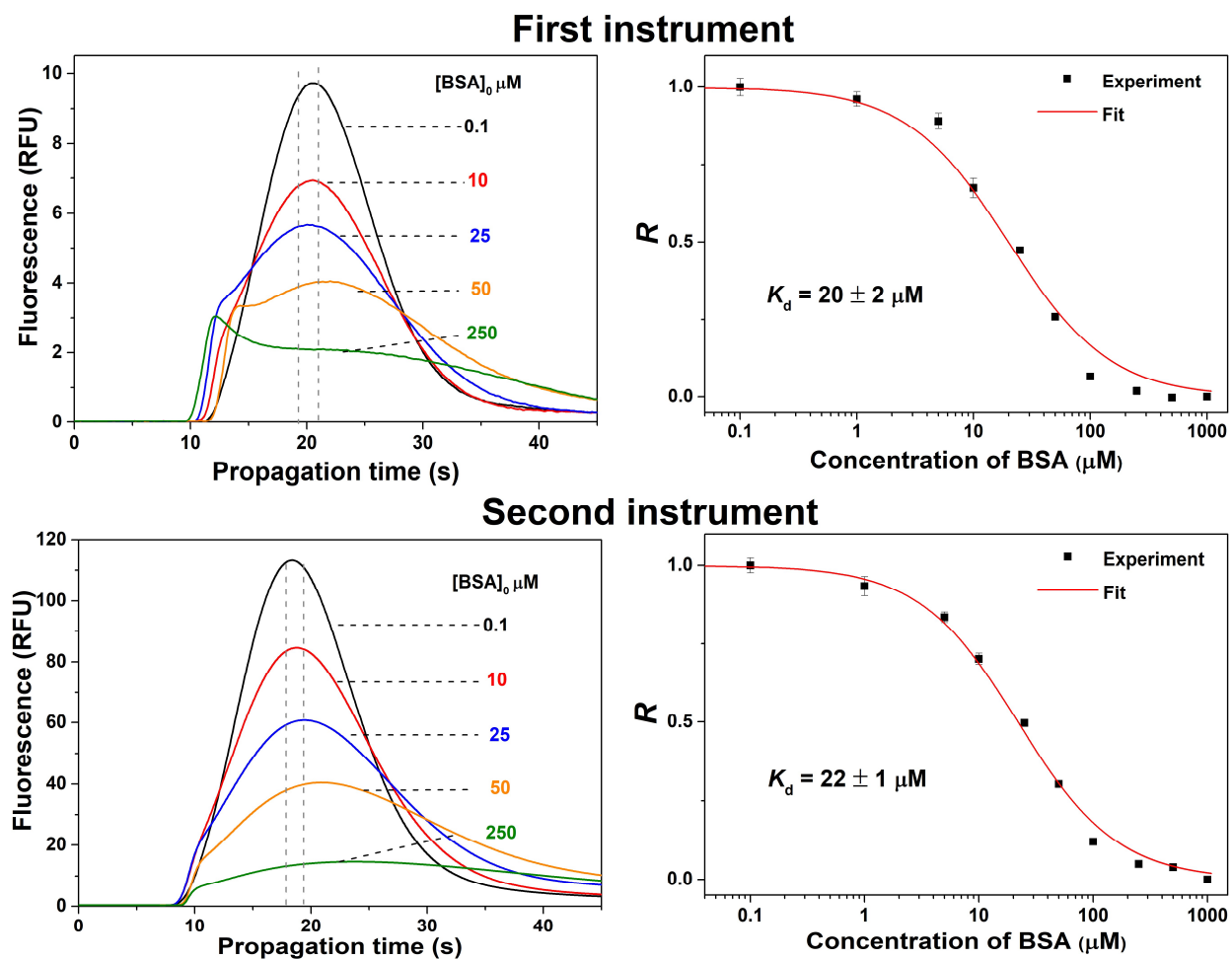


Figure S4: Determination of K_d Value of the BSA–Fluorescein Pair on Day 4

For the parallel experiments, identical samples containing 200 nM fluorescein and different concentrations of BSA were used. The left panels show representative separagrams for each concentration of BSA, and the right panels show the corresponding binding isotherms obtained for all of the separagrams. R is the fraction of unbound fluorescein.

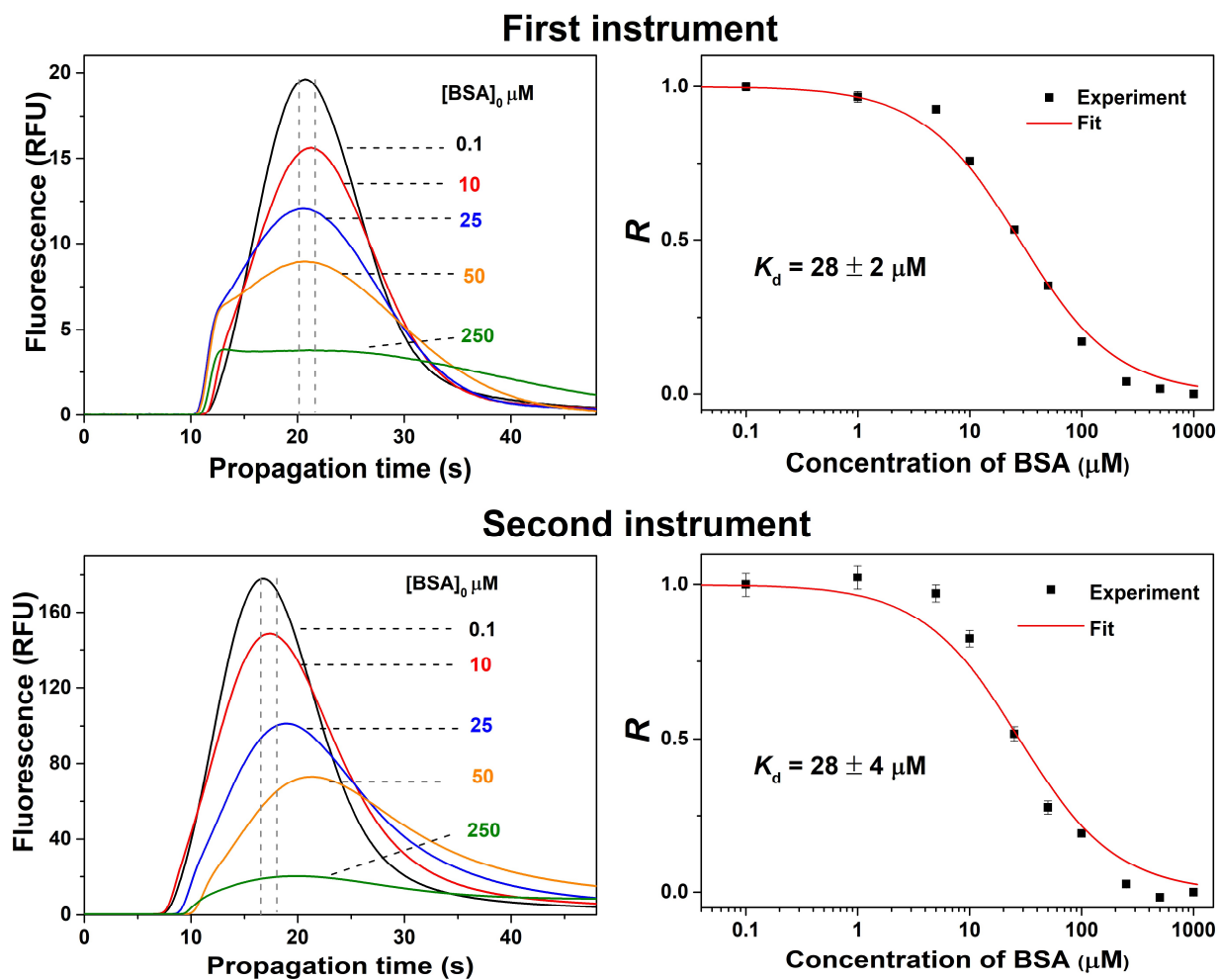


Figure S5: Determination of K_d Value of the BSA–Fluorescein Pair on Day 5

For the parallel experiments, identical samples containing 100 nM fluorescein and different concentrations of BSA were used. The left panels show representative separagrams for each concentration of BSA, and the right panels show the corresponding binding isotherms obtained for all of the separagrams. R is the fraction of unbound fluorescein. A new batch of BSA was used for this experiment, while all other experiments were performed with a single other batch.

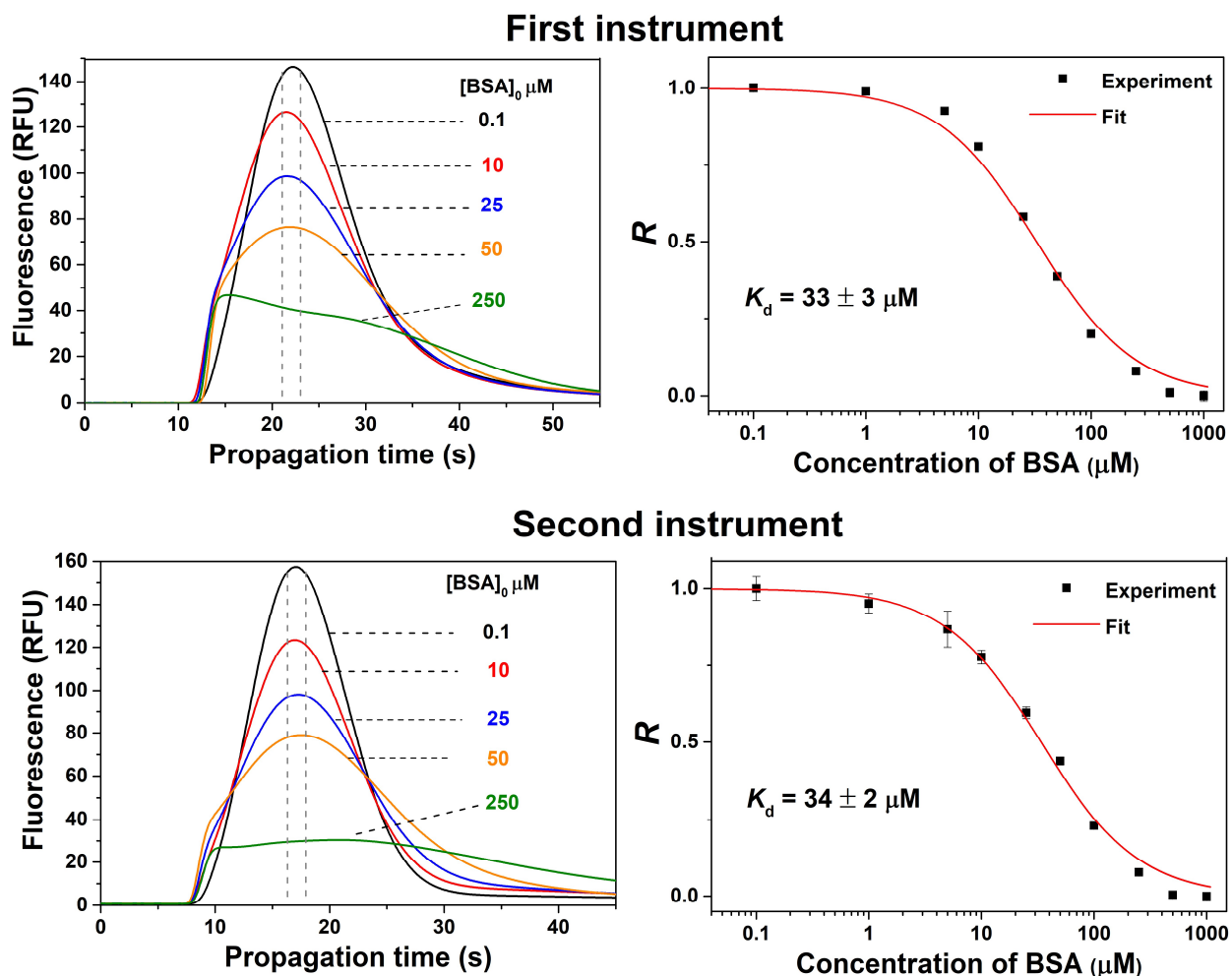


Figure S6: Repeatability of the ACTIS Separagrams for the BSA-Fluorescein Complex, Day 1, Instrument 1

For all the equilibrium mixtures, the total concentration of fluorescein was 100 nM, while the total concentrations of BSA varied from 0.1 to 1,000 μM as shown in the figure.

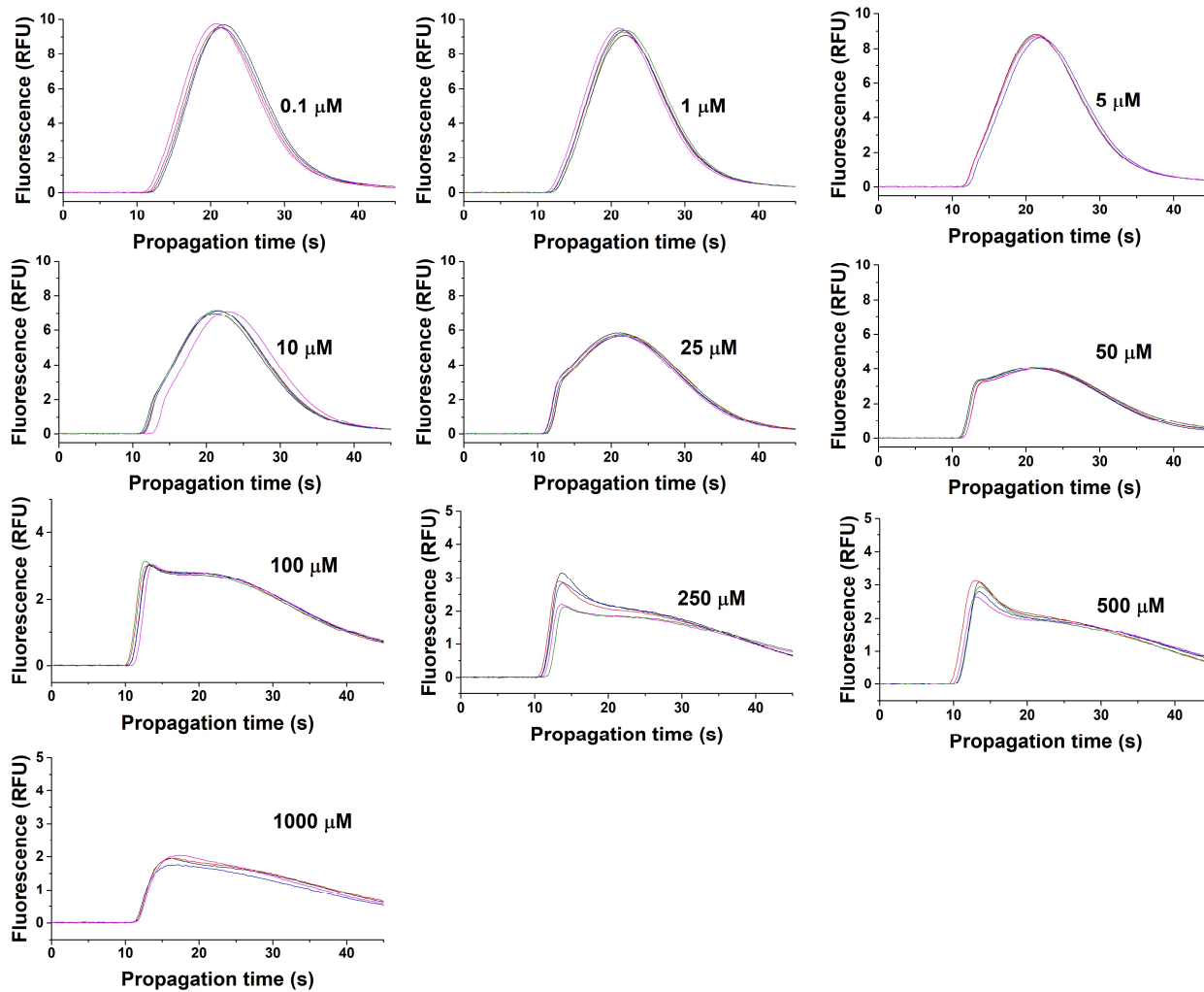


Figure S7: Repeatability of the ACTIS Separagrams for the BSA-Fluorescein Complex, Day 1, Instrument 2

For all the equilibrium mixtures, the total concentration of fluorescein was 100 nM, while the total concentrations of BSA varied from 0.1 to 1,000 μM as shown in the figure.

